Comparing methods for detection and quantification of plasmodesmal callose in *Nicotiana benthamiana* leaves during defense responses

Amie F. Sankoh[1,2], Joseph Adjei[2], Daniel M. Roberts[1] and Tessa M. Burch-Smith[2*]

[1]Department of Biochemistry & Cellular and Molecular Biology, The University of Tennessee, Knoxville, TN 37996 USA

[2]Donald Danforth Plant Science Center, Saint Louis, MO 63132 USA

*Corresponding author: Tessa M. Burch-Smith, TBurch-Smith@danforthcenter.org

Abstract

Callose, a beta-(1,3)-D-glucan polymer, is essential for regulating intercellular trafficking via plasmodesmata (PD). Pathogens manipulate PD-localized proteins to enable intercellular trafficking by removing callose at PD, or conversely by increasing callose accumulation at PD to limit intercellular trafficking during infection. Plant defense hormones like salicylic acid regulate PD-localized proteins to control PD and intercellular trafficking during immune defense responses such as systemic acquired resistance. Measuring callose deposition at PD in plants has therefore emerged as a popular parameter for assessing likely intercellular trafficking activity during plant immunity. Despite the popularity of this metric there is no standard for how these measurements should be made. In this study, we compared three commonly used methods for identifying and quantifying PD callose by aniline blue staining were evaluated to determine the most effective in the *Nicotiana benthamiana* leaf model. The results reveal that the most

reliable method used aniline blue staining and fluorescent microscopy to measure callose deposition in fixed tissue. Manual or semi-automated workflows for image analysis were also compared and found to produce similar results although the semi-automated workflow produced a wider distribution of data points.

Keywords: Aniline blue, callose, image analysis, plasmodesmata, salicylic acid

Main text

In plants, cell-to-cell communication is largely mediated by numerous small pores in the cell wall called plasmodesmata (PD) that directly connect the cytoplasms of neighboring cells (Kang et al., 2022). PD are essential for intercellular communication, plant development, and growth. In many instances PD trafficking is regulated by the controlled accumulation of the β-1,3-glucan, callose, in the cell wall surrounding plasmodesmal pores (Zavaliev et al., 2011; Sankoh and Burch-Smith, 2021). Callose deposition restricts intercellular trafficking, whereas callose degradation increases intracellular trafficking. The restriction of PD trafficking likely occurs during defense against pathogens through the physical closure of the PD pore by the accumulation of callose (Zavaliev et al., 2011; Singh et al., 2017).

Plant hormones regulate PD callose levels to adjust intercellular trafficking. Exogenous application of salicylic acid (SA) to plants activates immune responses with a concomitant induction of callose accumulation at PD that lowers PD-mediated intercellular trafficking. SA induces the activity of PLASMODESMATA LOCATED PROTEIN (PDLP)5-directed machinery that induces callose accumulation and closes PD during immune responses (Lee and Lu, 2011; Lee et al., 2011). Local pathogen infection

often leads to resistance in systemic healthy, uninfected tissues by a process termed systemic acquired resistance (SAR). Systemic transport of SA is important for SAR, although it is transported in the apoplast and not via intercellular transport through PD (Lim 2016; Lim, 2020; Kachroo and Kachroo, 2020). In contrast to SA, other SAR signaling molecules like azelaic acid (AzA) and glycerol-3-phosphate (G3P) move systemically via PD (Lim et al., 2016). The importance of PD in SAR was highlighted by the observation of defective SAR in *pdlp1* and *pdlp5* mutants (Lim et al., 2016). This is proposed to result from altered PD permeability due to altered callose metabolism (Lee et al., 2011; Caillaud et al., 2014). SAR is also linked with the enhanced levels of callose accumulation upon secondary pathogen inoculation (Lee and Hwang, 2005; Conrath, 2006). Thus, many of SA's roles in immunity may link to its role in regulating PD via callose metabolism.

Given the importance of callose to regulating PD trafficking, it has become common practice to measure PD callose levels, for example, in response to pathogen infection as a gauge of the plant's response to infection. Because of its ability to bind callose (β-1,3-glucan), cellulose, and related polysaccharides in the cell walls, aniline blue has been widely adopted for visualization of callose deposition at PD (recent examples include (Huang et al., 2022; Muller et al., 2022; Yan, 2022)). We noticed that procedures for measuring PD callose varied between labs, with important differences in how samples were treated before application of aniline blue. In several studies, samples were fixed before staining (e.g. (Lee and Hwang, 2005; Lee et al., 2011; Zavaliev and Epel, 2015)), while in others aniline blue was introduced into living tissues without fixation (e.g. (Caillaud et al., 2014; Muller et al., 2022; Rocher et al., 2022). Because of these disparate

protocols, potential issues arise when comparing studies that use different staining approaches. The purpose of the present study was to determine which aniline blue staining approach was most reliable when used with leaves from *Nicotiana benthamiana*, a widely used model for plant-pathogen interactions (Goodin et al., 2008). For this purpose, three representative protocols were tested to identify the most reliable protocol for callose staining with aniline blue in *N. benthamiana* leaves.

The LAB cultivar of *N. benthamiana* was used in this study (Naim et al., 2012; Bally et al., 2015). Seedlings were germinated on soil for 7-10 days before transplanting to individual pots and plants were grown on light carts under long day conditions with 16 hours light (120 µmol m^{-2} s^{-1}) and 8 hours dark at 25 °C. Miracle Gro All-purpose Plant Food fertilizer was applied after 10-13 days post germination (3 days after transplanting). The leaves of 4-5-week-old plants were used for callose quantification and SA-treatment experiments.

The first protocol for callose staining we tested, Method 1, was adapted from the Epel lab (Zavaliev and Epel, 2015). An entire cut leaf was submerged in 95-96% ethanol in a 500-mL polypropylene jar to fix and bleach the tissue. The petiole was held with forceps to avoid mechanical damage to the leaf. The jar was sealed, and samples were incubated at room temperature on a shaker at 30-40 rpm for at least 5 hours. The ethanol solution was changed after 2 hours incubation to accelerate tissue bleaching. Incubation was continued until the leaves were completely or nearly completely bleached, but less than 6 hours, since even more severe tissue damage occurred after this point compared to the mild tissue damage we observed (Fig. 1A and B). Incubating plant cells in 95-99% ethanol for more than six hours likely damaged the tissue since ethanol is a dehydrating

agent and high concentrations of ethanol can cause water to leave the cell, while also disrupting the structure of cell membranes. Bleached leaves were removed and were placed in a petri dish and cut into 5 mm wide strips with a razor blade. The cut strips were rehydrated in double distilled water (DDW) with 0.01% (v/v) Tween-20 and incubated at room temperature for 1 hour on a shaker at 30-40 rpm. Tissues were then transferred to a small petri dish (35mm in diameter and 10 mm height) and submerged in 1% (w/v) aniline blue (Ward's Science plus, Rochester NY LOT AD-22103) in 0.01 M K_3PO_4, pH 12. The uncovered petri dish was placed in a desiccator under house vacuum for approximately 10 minutes followed by slow release of pressure. The petri dish was covered and sealed with foil before shaking at room temperature for 2 hours at 30-40 rpm. The samples were then directly imaged without destaining with a Leica SP8 laser scanning confocal microscope (Leica, Whetzlar, Germany).

Callose deposits in the abaxial side of the leaves were imaged using a 40x/1.10 water immersion objective (HC PL APO CS2 40x/1.10 WATER). The excitation for aniline blue was carried out with a 405-nm laser, UV (0.5-1%) and emission was captured from 415 nm-525 nm. Z-stacks were collected from multiple regions of interest (ROI; approximately 23-25 ROIs per leaf) using the system optimized step size (<1 µm). To observe as many PD as possible, the pinhole aperture was initially set to open before being adjusted to approximately 1 Airy unit for image collection. Laser intensity and gain were adjusted to optimize the PD fluorescence against the background signal, while being careful to avoid oversaturation of callose sites. Twenty-three to twenty-five Z-stacks were imaged using the same settings of image acquisition in the independent experiments.

Because individual PD cannot be resolved by light microscopy, individual aniline blue-stained foci likely represent multiple PD arranged into groups (within pitfields) rather than individual PD, we refer to these foci as “clusters of PD”. We measured the number of aniline-blue stained clusters of PD, which are concentrated areas of high PD density between 0.05 μm^2 and 4 μm^2 in size. A representative maximum intensity projection of a z-stack from confocal microscopy of the untreated control are shown (Fig. 1A). They show multiple clusters of PD in the cell wall, and other artifacts that are not within the cell wall (marked with white arrows).

The other methods employed involved the direct staining of plant tissue without a prior fixation step. The aniline blue staining solution and confocal microscopy imaging protocols were the same as those used for Method 1. Method 2 was adapted from a protocol available at https://www.jic.ac.uk/research-impact/aniline-blue-staining-of-qunatification-of-plasmodesmal-callose/ (Faulkner et al., 2013; Xu et al., 2017). Staining involved direct infiltration of 1% (w/v) aniline blue into leaves using a 1-mL needleless syringe while they were still attached to the plants. Infiltrated leaves were cut into 1 cm^2 squares, and clusters of PD were observed under the confocal microscope away from the cutting site to avoid sites of wound-induced callose deposition. A representative maximum intensity projection of a z-stack without SA treatment is shown (Fig. 1C). Aniline blue foci representing clusters of PD were clearly observed in the cell wall, and staining of other structures were rarely observed.

Method 3 was adapted from the Lee lab (Cui and Lee, 2016). Leaves were cut into 5 mm strips and incubated in 1% (w/v) aniline blue in 0.01 M K_3PO_4, pH 12 in darkness for 30-60 minutes. A representative image is shown (Fig. 1E). Similar to Method 2, aniline

blue-stained foci were only detected in the cell wall, and few, if any, other cellular structures were stained (Fig. 1A-C).

To determine the average density of clusters of PD per unit cell wall, at least 25 z-stacks were collected from three to four biological replicates for each method, and analysis was performed using ImageJ Fiji (Schindelin et al., 2012). Clusters of PD were quantified per 100 μm^2 of cell wall for a region of interest. The number of clusters of PD was selected as the parameter for measuring callose accumulation since we and others have found that the fluorescence intensity of aniline blue-stained PD callose may not accurately reflect alterations in callose deposition. For example, the number of aniline blue-stained foci was found to be a more reliable indicator of changes in callose deposition at PD compared to fluorescence intensity alone (Dmitrieva et al. 2017). The workflow of the analysis for counting the number of aniline-blue stained clusters of PD is presented in the Supplementary Materials (Fig. S1 using the data presented in Fig. 1A). The first step in the image analysis workflow was to convert the maximum intensity projection to 8-bit (Fig. S1). The image was then inverted to perform inverse binary thresholding to measure the area of clusters of PD shown in red spots (Fig. S1). Cell-wall lengths were measured by tracing the cell wall in the region of interest (Fig. S1). Only the total number of clusters of PD within the traced cell walls was calculated within each region of interest as clusters of PD/unit area (Fig. S1). We first measured the number of clusters of PD in untreated control plant cell walls using each method to clearly discern the variation between biological replicates (Fig. 2). The colors represent data points from various biological replicates. An interquartile range (IQR) analysis was used to identify

and exclude outlier data points more than 1.5 times the interquartile range (Fig. 2B). All three methods display similar medians in the control plants.

SA can reduce intercellular trafficking via PD during immune response against pathogens (Koo et al., 2020). To compare the various methods for the quantitation of the accumulation of callose at PD induced by SA, *N. benthamiana* leaves were infiltrated with 0.05 mM SA dissolved in DMSO and diluted in water, and after 12 hours the leaves were stained with aniline blue using each of the three previously described methods. Representative images of SA-treated samples are shown for each method (Fig. 1B,D,F). A comparison of the density of clusters of PD in control and SA-treated plants from multiple experiments is shown in Fig. 3. (Individual replicates are presented in Fig. S3). For the sake of comparison, we normalized the SA treatment data to the average control group within each replicate. For Method 1, each replicate showed an increase in PD callose, reflected as an increase in PD cluster density, with median density increasing from 3.4 to 5.7 on treatment with SA ($p<0.0005$; Fig. 3A). For method 2, however, the experimental replicates did not consistently show increased callose at PD in response to SA treatment (Fig. 3B). This inconsistency is best exemplified by Replicate 2 (green dots) and Replicate 4 (black dots), which show no change or a decrease in PD cluster density upon SA application, respectively. It is worth noting that applying IQR analysis to the datasets resulted in a change in the statistical significance of the results obtained with method 2, with no significant difference before IQR analysis compared to a statistically significant difference after elimination of outlying data points by IQR analysis (compare Fig. S2 to Fig. 3). Method 3 showed a similar inconsistency with significant differences between the control and SA-treated plants only observed for one biological replicate

(Replicate 2 in Fig. 3C). The median density of clusters of PD increased from 3.2 to 4.6 on treatment with SA ($p<0.0005$). Thus, the three methods showed distinct sensitivity and reproducibility/consistency when comparing SA-induced aniline blue stained PD foci (Fig. 3).

We then determined the fold induction of callose, and the range and standard deviation of data points (Fig. 3D). Comparison of the data show that Method 1 had the smallest range of values (0.33 to 2.7), with a lower occurrence of outliers and the lowest standard deviation (0.08). Data points from each replicate are distributed evenly for Method 1, whereas data points for each replicate in Methods 2 and 3 are more widely distributed over a greater range with more outliers (Fig. 3B-D). Taken together, the data show that Method 1 generates more consistent experimental results for each biological replicate with fewer outliers compared to the higher variability observed with Methods 2 and 3.

The generation of the data shown in Fig. 3 relies upon manual image analysis using ImageJ which is labor intensive. To evaluate whether the process could be automated, we compared the results from the manual workflow to CalloseQuant, a plug-in for semi-automated image analysis for image and quantification of callose at PD (Huang, 2022). The CalloseQuant plug-in offers two methods; CalloseQuant A is highly sensitive to fluorescence intensity whereas CalloseQuant B has low sensitivity because of thresholding, which makes it especially susceptible to the presence of fluorescence (organelles) outside the ROI and outside the cell wall area (Huang, 2022). Here, both CalloseQuant approaches were compared with the callosequant.ijm plugin for ImageJ using the images generated by callose staining Method 1 (Fig. 4).

Images captured using confocal microscopy were first auto-scaled and converted into .tiff format using FIJI ImageJ. For the series of confocal micrographs analyzed, the peak prominence values ranges were between 25-45 µm, and the measurement radius was maintained at 5.5 for CalloseQuant A. For CalloseQuant B, the rolling ball radius range was used with 6-8 pixels, and the mean filter radius was kept at 2 pixels. We optimized other parameters described in (Huang et al., 2022) to ensure only PD-associated aniline blue foci were included in the analysis. All the data collected were manually checked for the elimination of signals and data points outside of the region of interest (ROI). A comparison of densities of clusters of PD calculated from our manual and the semi-automated CalloseQuant workflows is shown in Fig. 4. All three analytical approaches generated datasets that show a statistically significant induction of PD callose by SA treatment. However, the median value obtained with the semiautomated approaches were lower than the manual approach and showed a wider distribution and range of data with outliers. 2D images with lower magnification are recommended for use with CalloseQuant (Huang et al., 2022). However, z-stacks (3D) images like those used in our manual workflow gave more details on lusters of PD in the z-axis. When z-stacks are combined with binary watershed segmentation (which separates closely adjacent foci) a better estimation of the number of aniline blue-stained foci is likely to be obtained.

The side-by-side comparison of three methods for staining tissues for the presence of callose at PD found that fixation of *N. benthamiana* leaf tissue prior to aniline blue staining produced the most reproducible results with similar increases in callose levels on treatment with SA, (Fig. 3A and D). A comparison of manual and semi-automated analytic

workflows for quantification of aniline blue-stained foci in confocal images revealed similar performance but with manual analysis a giving smaller distribution of PD density values. For high-throughput studies, the semi-automated PD quantification tool will clearly benefit the field. Recently, the use of Ilastik supervised machine learning imagery data collection software for measuring callose levels in the phloem has been reported (Welker and Levy, 2022). This approach was shown to be more reliable than the approaches using ImageJ Fiji than our manual analysis and CalloseQuant workflows. In the future, use of new analytical pipelines like those of Welker and Levy (Welker and Levy, 2022) will undoubtedly improve the quality of data regarding PD callose accumulation during defense.

Acknowledgements

We thank Dr. Kirk Czymmek and staff of the Donald Danforth Plant Science Center Advanced Bioimaging Lab for assistance with microscopy and Dr. Brandon Reagan, Michigan State University, for guidance on image analysis. This work was supported by NSF award MCB 2210127 to T.B.-S. and an NIH pre-doctoral fellowship 1F31GM148051-01 to A.F.S.

Literature Cited

Bally, J., Nakasugi, K., Jia, F., Jung, H., Ho, S.Y., Wong, M., Paul, C.M., Naim, F., Wood, C.C., Crowhurst, R.N., Hellens, R.P., Dale, J.L., and Waterhouse, P.M. 2015. The extremophile Nicotiana benthamiana has traded viral defence for early vigour. Nat Plants 1:15165.

Caillaud, M.C., Wirthmueller, L., Sklenar, J., Findlay, K., Piquerez, S.J., Jones, A.M., Robatzek, S., Jones, J.D., and Faulkner, C. 2014. The plasmodesmal protein PDLP1 localises to haustoria-associated membranes during downy mildew infection and regulates callose deposition. PLoS pathogens 10:e1004496.

Conrath, U. 2006. Systemic acquired resistance. Plant Signal Behav 1:179-184.

Cui, W., and Lee, J.Y. 2016. Arabidopsis callose synthases CalS1/8 regulate plasmodesmal permeability during stress. Nat Plants 2:16034.

Dmitrieva, V.A., Domashkina, V.V., Ivanova, A.N., Sukhov, V.S., Tyutereva, E.V., and Voitsekhovskaja, O.V. 2021. Regulation of plasmodesmata in Arabidopsis leaves: ATP, NADPH and chlorophyll b levels matter. J Exp Bot 72:5534-5552.

Faulkner, C., Petutschnig, E., Benitez-Alfonso, Y., Beck, M., Robatzek, S., Lipka, V., and Maule, A.J. 2013. LYM2-dependent chitin perception limits molecular flux via plasmodesmata. Proc Natl Acad Sci U S A 110:9166-9170.

Goodin, M.M., Zaitlin, D., Naidu, R.A., and Lommel, S.A. 2008. Nicotiana benthamiana: its history and future as a model for plant-pathogen interactions. Mol Plant Microbe Interact 21:1015-1026.

Huang, C., Mutterer, J., and Heinlein, M. 2022. In Vivo Aniline Blue Staining and Semiautomated Quantification of Callose Deposition at Plasmodesmata. Methods Mol Biol 2457:151-165.

Kachroo, A., and Kachroo, P. 2020. Mobile signals in systemic acquired resistance. Curr Opin Plant Biol 58:41-47.

Kang, B.H., Anderson, C.T., Arimura, S.I., Bayer, E., Bezanilla, M., Botella, M.A., Brandizzi, F., Burch-Smith, T.M., Chapman, K.D., Dunser, K., Gu, Y., Jaillais, Y.,

Kirchhoff, H., Otegui, M.S., Rosado, A., Tang, Y., Kleine-Vehn, J., Wang, P., and Zolman, B.K. 2022. A glossary of plant cell structures: Current insights and future questions. Plant Cell 34:10-52.

Koo, Y.M., Heo, A.Y., and Choi, H.W. 2020. Salicylic Acid as a Safe Plant Protector and Growth Regulator. Plant Pathol J 36:1-10.

Lee, J.Y., and Lu, H. 2011. Plasmodesmata: the battleground against intruders. Trends Plant Sci 16:201-210.

Lee, J.Y., Wang, X., Cui, W., Sager, R., Modla, S., Czymmek, K., Zybaliov, B., van Wijk, K., Zhang, C., Lu, H., and Lakshmanan, V. 2011. A plasmodesmata-localized protein mediates crosstalk between cell-to-cell communication and innate immunity in Arabidopsis. Plant Cell 23:3353-3373.

Lee, S.C., and Hwang, B.K. 2005. Induction of some defense-related genes and oxidative burst is required for the establishment of systemic acquired resistance in Capsicum annuum. Planta 221:790-800.

Lim, G.H., Shine, M.B., de Lorenzo, L., Yu, K., Cui, W., Navarre, D., Hunt, A.G., Lee, J.Y., Kachroo, A., and Kachroo, P. 2016. Plasmodesmata Localizing Proteins Regulate Transport and Signaling during Systemic Acquired Immunity in Plants. Cell Host Microbe 19:541-549.

Muller, A., Fujita, T., and Coudert, Y. 2022. Callose Detection and Quantification at Plasmodesmata in Bryophytes. Methods Mol Biol 2457:177-187.

Naim, F., Nakasugi, K., Crowhurst, R.N., Hilario, E., Zwart, A.B., Hellens, R.P., Taylor, J.M., Waterhouse, P.M., and Wood, C.C. 2012. Advanced engineering of lipid

metabolism in Nicotiana benthamiana using a draft genome and the V2 viral silencing-suppressor protein. PloS one 7:e52717.

Rocher, M., Simon, V., Jolivet, M.D., Sofer, L., Deroubaix, A.F., Germain, V., Mongrand, S., and German-Retana, S. 2022. StREM1.3 REMORIN Protein Plays an Agonistic Role in Potyvirus Cell-to-Cell Movement in N. benthamiana. Viruses 14.

Sankoh, A.F., and Burch-Smith, T.M. 2021. Approaches for investigating plasmodesmata and effective communication. Curr Opin Plant Biol 64:102143.

Schindelin, J., Arganda-Carreras, I., Frise, E., Kaynig, V., Longair, M., Pietzsch, T., Preibisch, S., Rueden, C., Saalfeld, S., Schmid, B., Tinevez, J.Y., White, D.J., Hartenstein, V., Eliceiri, K., Tomancak, P., and Cardona, A. 2012. Fiji: an open-source platform for biological-image analysis. Nature methods 9:676-682.

Singh, A., Lim, G.H., and Kachroo, P. 2017. Transport of chemical signals in systemic acquired resistance. J Integr Plant Biol 59:336-344.

Welker, S., and Levy, A. 2022. Comparing Machine Learning and Binary Thresholding Methods for Quantification of Callose Deposits in the Citrus Phloem. Plants 11.

Xu, B., Cheval, C., Laohavisit, A., Hocking, B., Chiasson, D., Olsson, T.S.G., Shirasu, K., Faulkner, C., and Gilliham, M. 2017. A calmodulin-like protein regulates plasmodesmal closure during bacterial immune responses. The New phytologist 215:77-84.

Yan, D. 2022. Spatiotemporal Specific Blocking of Plasmodesmata by Callose Induction. Methods Mol Biol 2457:383-391.

Zavaliev, R., and Epel, B.L. 2015. Imaging callose at plasmodesmata using aniline blue: quantitative confocal microscopy. Methods Mol Biol 1217:105-119.

Zavaliev, R., Ueki, S., Citovsky, V., and Epel, B.L. 2011. Biology of callose (beta-1,3-glucan) turnover at plasmodesmata. Protoplasma 248:117-130.

Figure captions

Figure 1. Results from the three methods of aniline blue staining for imaging clusters of PD

N. benthamiana leaf epidermal cells with staining of PD callose using 1% aniline blue solution. Representative images are shown for three different callose staining methods, both for untreated and SA treated plants. **A**, Method 1 using fixed tissue with white arrows indicating artifacts that are not within the cell wall. **B,** Method 1 in tissue treated with 0.05 mM SA for 12 hours. **C,** Method 2 using non-fixed tissue directly infiltrated with aniline blue. **D,** Method 2 in 0.05 mM SA-treated tissues. **E,** Method 3 using non-fixed tissue stained with aniline blue for 30-60 minutes. **F,** Method 3 in 0.05 mM SA-treated tissues. Images are maximum projections of Z-stacks of images collected by confocal fluorescence microscopy. Scale bars = 10 μm.

Figure 2. Reproducibility of quantification of clusters of PD across methods in untreated control plants

A, The PD cluster quantification data from 3-4 biological replicates are shown by box and whisker plot. Three replicates were used for Methods 1 and 3 while four replicates were collected for Method 2. **B,** The same data shown in **A** is replotted using IQR analysis to remove outliers from each replicate. Median values of clusters of PD per 100 μm^2 of cell wall (red text) are displayed above each plot. Medians from all methods are not significantly different from each other based on the Tukey's multiple comparisons test. P-values for method 1 vs. method 2 combination = 0.5037; method 1 vs. method 3 = 0.9915 and method 2 vs method 3 = 0.4271.

Figure 3. Quantification of PD callose in *N. benthamiana* leaves treated with 0.05 mM salicylic acid (SA) to induce callose.

PD cluster densities were quantified for at least 23 regions of interest (ROIs) for each replicate and each replicate is represented by a different color. **A,** Three (3) biological replicates prepared by Method 1 after 12 hours SA treatment. **B,** Four (4) biological replicates prepared by Method 2 after 12 hours SA treatment. **C,** Three (3) biological replicates prepared by Method 3 after 12 hours SA treatment. Statistical significance of each treatment compared to the control was determined by the Welch's unequal variances t-test (**** means $p<0.0001$). **D,** Fold induction by SA for all three methods along with the standard deviation, standard error and range. Clusters of PD per 100 μm^2 cell wall were normalized to untreated control.

Figure 4. Comparison of manual and automated (CalloseQuant) methods for quantifying callose PD accumulation. A, Aniline blue-stained images of untreated or SA-treated samples prepared using Method 1 (fixation) were quantified using manual counting in ImageJ, CalloseQuant A, or CalloseQuant B. Three biological replicates are shown using different colors. **B,** The fold induction of callose in response to SA treatment, standard deviation, standard error and range are shown. Statistical significance was determined by Welch's t-test (**** means $p<0.0001$).

e-Xtra Figure captions

Fig. S1. Using FIJI to manually quantify the number of clusters of PD and measure the cell length (area). Maximum intensity projections of a Z-stack of images (**A**) were converted to 8 bit (**B**), inverted (**C**), and a threshold was set to select callose staining (red; **D**) along the cell wall. Adjoining foci were separated to distinct bodies using binary watershed (**E)**. Any signal that is not along the cell wall was manually excluded (**F, G**). Lastly, the length of cell wall within ROI was measured using the segmented line tool (**H**). An automatic particle analysis was performed to obtain information on PD-associated callose particles. Clusters of PD per 100 μm^2 cell wall were calculated using Microsoft Excel.

Fig. S2 Quantification of numbers of clusters of PD for each method using all data, without IQR analysis. Quantification of staining of callose depositions with 1% aniline blue in untreated leaves and after 12 hours salicylic acid (SA) treatment. **A**, Method 1 shows a significant difference (p=0.0001), **B**, Method 2 show no significant difference (p=0.0705), and **C**, Method 3 shows a significant difference (p=0.0014) using the Welch's t-test (ns = not significant, ** = p≤0.01; ***, p≤0.001).

Fig. S3 Individual replicates for samples with or without treatment with SA. The fold change in the density of clusters of PD for each replicate is indicated before each graph. The data are the disaggregated data presented in Fig. 3 in the main text. Statistical analysis, Welch's t-test, was performed as described in the caption of Fig. 3.

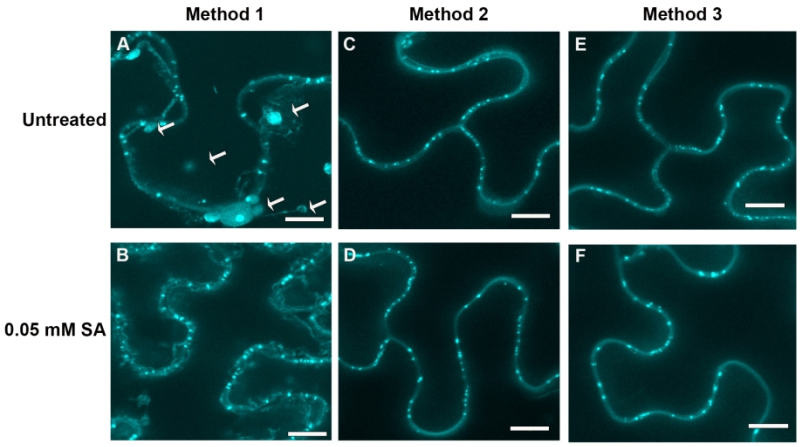

Fig.1

Figure 1. Results from the three methods of aniline blue staining for PD cluster imaging
N. benthamiana leaf epidermal cells with staining of PD callose using 1% aniline blue solution. Representative images are shown for three different callose staining methods, both for untreated and SA treated plants. A, Method 1 using fixed tissue with white arrows indicating artifacts that are not within the cell wall. B, Method 1 in tissue treated with 0.05 mM SA for 12 hours. C, Method 2 using non-fixed tissue directly infiltrated with aniline blue. D, Method 2 in 0.05 mM SA-treated tissues. E, Method 3 using non-fixed tissue stained with aniline blue for 30-60 minutes. F, Method 3 in 0.05 mM SA-treated tissues. Images are maximum projections of Z-stacks of images collected by confocal fluorescence microscopy. Scale bars = 10 µm.

215x279mm (300 x 300 DPI)

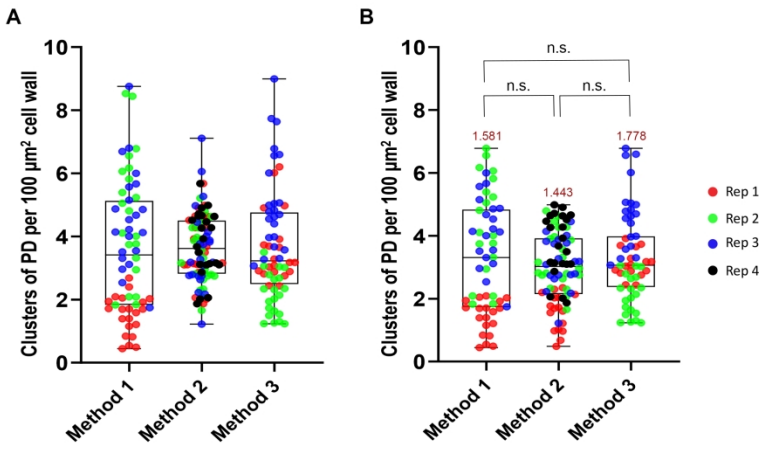

Fig. 2

Figure 2. Reproducibility of quantification of clusters of PD across methods in untreated control plants
A, The PD cluster quantification data from 3-4 biological replicates are shown by box and whisker plot. Three replicates were used for Methods 1 and 3 while four replicates were collected for Method 2. B, The same data shown in A is replotted using IQR analysis to remove outliers from each replicate. Median values of clusters of PD per 100 µm2 of cell wall (red text) are displayed above each plot. Medians from all methods are not significantly different from each other based on the Tukey's multiple comparisons test. P-values for method 1 vs. method 2 combination = 0.5037; method 1 vs. method 3 = 0.9915 and method 2 vs method 3 = 0.4271.

215x279mm (300 x 300 DPI)

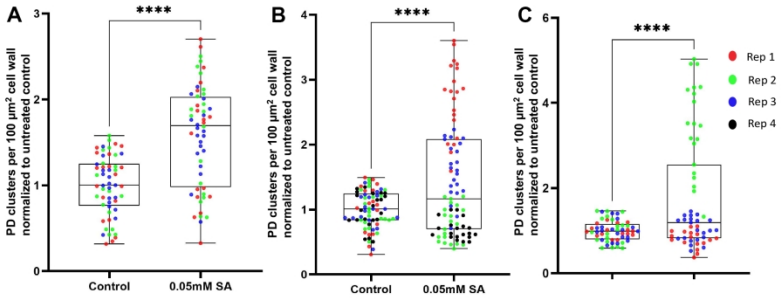

D

	Fold induction by SA	Std. Deviation	Std. Error of Mean	Range of SA	Difference in Range
Method 1	1.58	0.59	0.08	0.33 - 2.70	2.37
Method 2	1.44	0.89	0.097	0.4 - 3.6	3.20
Method 3	1.78	1.4	0.177	0.37 - 5.03	4.66

Fig. 3

Figure 3. Quantification of PD callose in N. benthamiana leaves treated with 0.05 mM salicylic acid (SA) to induce callose.
PD cluster densities were quantified for at least 23 regions of interest (ROIs) for each replicate and each replicate is represented by a different color. A, Three (3) biological replicates prepared by Method 1 after 12 hours SA treatment. B, Four (4) biological replicates prepared by Method 2 after 12 hours SA treatment. C, Three (3) biological replicates prepared by Method 3 after 12 hours SA treatment. Statistical significance of each treatment compared to the control was determined by the Welch's unequal variances t-test (**** means $p<0.0001$). D, Fold induction by SA for all three methods along with the standard deviation, standard error and range. PD clusters per 100 µm2 cell wall were normalized to untreated control.

215x279mm (300 x 300 DPI)

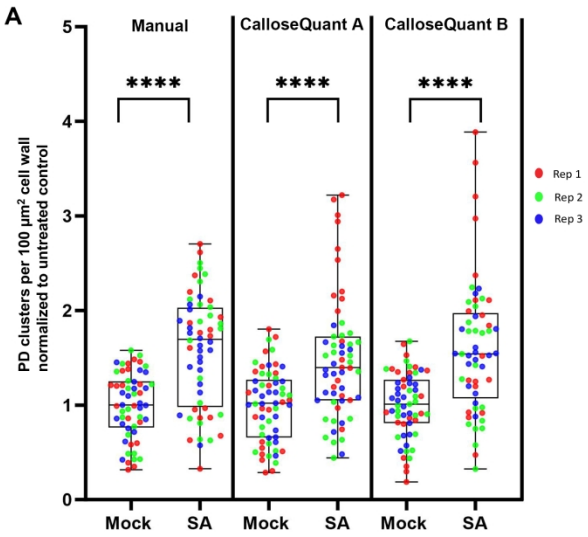

B

	Fold induction by SA	Std. Deviation	Std. Error of Mean	Range
Manual	1.58	0.5959	0.07963	0.326 - 2.703
CalloseQuant A	1.48	0.6451	0.08398	0.441 - 3.221
CalloseQuant B	1.60	0.7086	0.09386	0.325 - 3.885

Fig. 4

Figure 4. Comparison of manual and automated (CalloseQuant) methods for quantifying callose PD accumulation. A, Aniline blue-stained images of untreated or SA-treated samples prepared using Method 1 (fixation) were quantified using manual counting in ImageJ, CalloseQuant A, or CalloseQuant B. Three biological replicates are shown using different colors. B, The fold induction of callose in response to SA treatment, standard deviation, standard error and range are shown. Statistical significance was determined by Welch's t-test (**** means $p<0.0001$).

215x279mm (300 x 300 DPI)

Sankoh, A.F.

e-Xtra

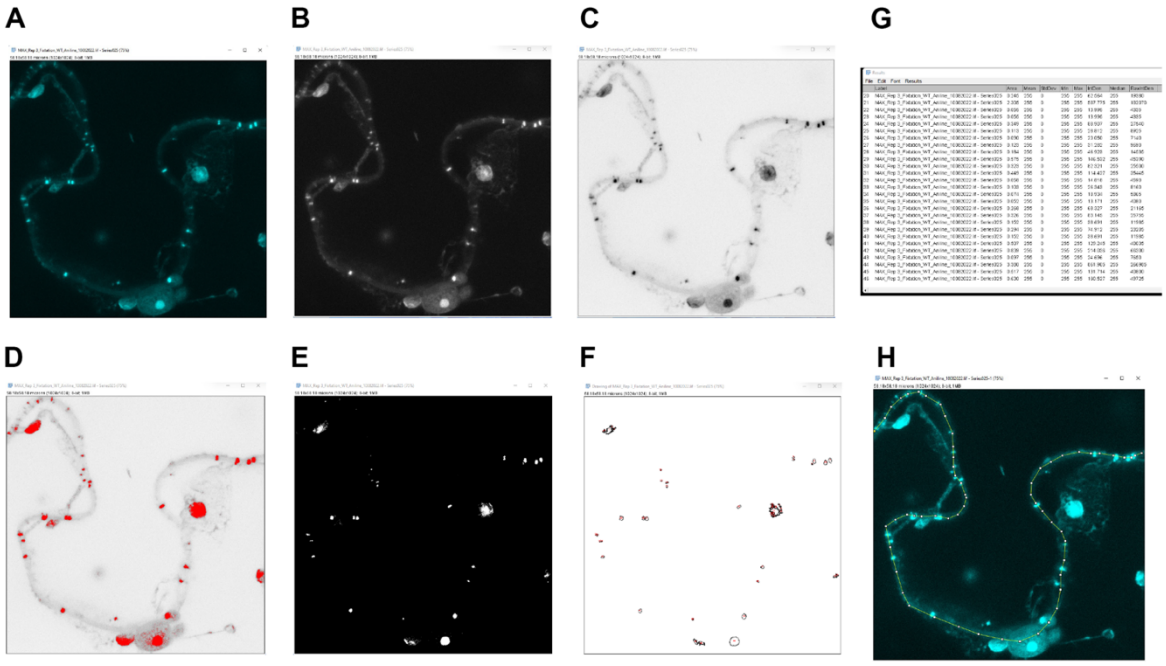

Fig. S1. Using FIJI to manually quantify the number of clusters of PD and measure the cell length (area). Maximum intensity projections of a Z-stack of images (**A**) were converted to 8 bit (**B**), inverted (**C**), and a threshold was set to select callose staining (red; **D**) along the cell wall. Adjoining foci were separated to distinct bodies using binary watershed (**E**). Any signal that is not along the cell wall was manually excluded (**F, G**). Lastly, the length of cell wall within ROI was measured using the segmented line tool (**H**). An automatic particle analysis was performed to obtain information on PD-associated callose particles. Clusters of PD per 100 μm^2 cell wall were calculated using Microsoft Excel.

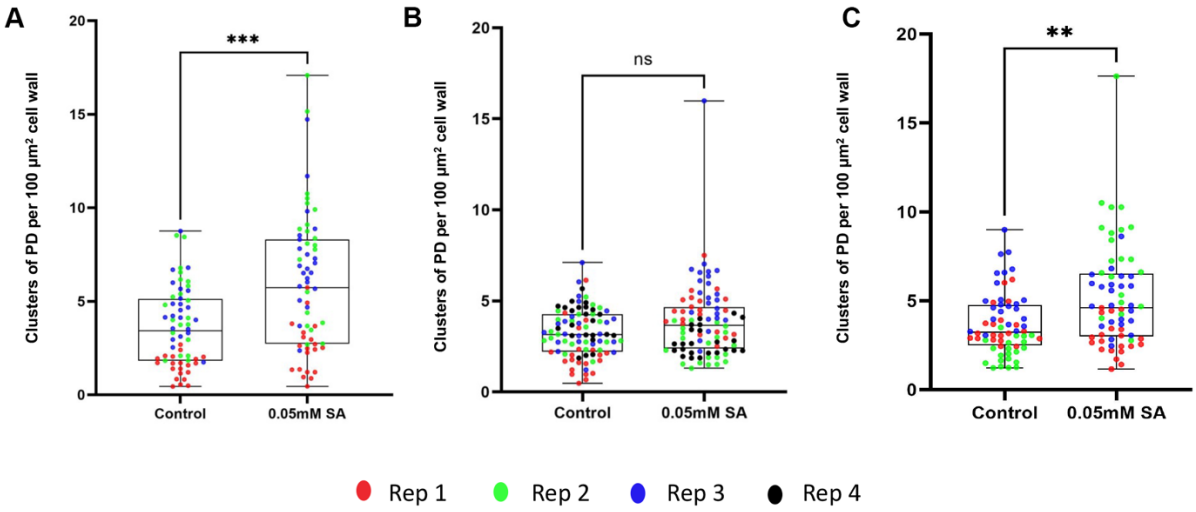

Fig. S2. Quantification of numbers of clusters of PD for each method using all data, without IQR analysis. Quantification of staining of callose deposition with 1% aniline blue in untreated leaves and after 12 hours salicylic acid (SA) treatment. **A**, Method 1 showed a significant difference (p=0.0001), **B**, Method 2 showed no significant difference (p=0.0705), and **C**, Method 3 showed a significant difference (p=0.0014) using the Welch's t-test (ns = not significant, ** = p≤0.01; ***, p≤0.001).

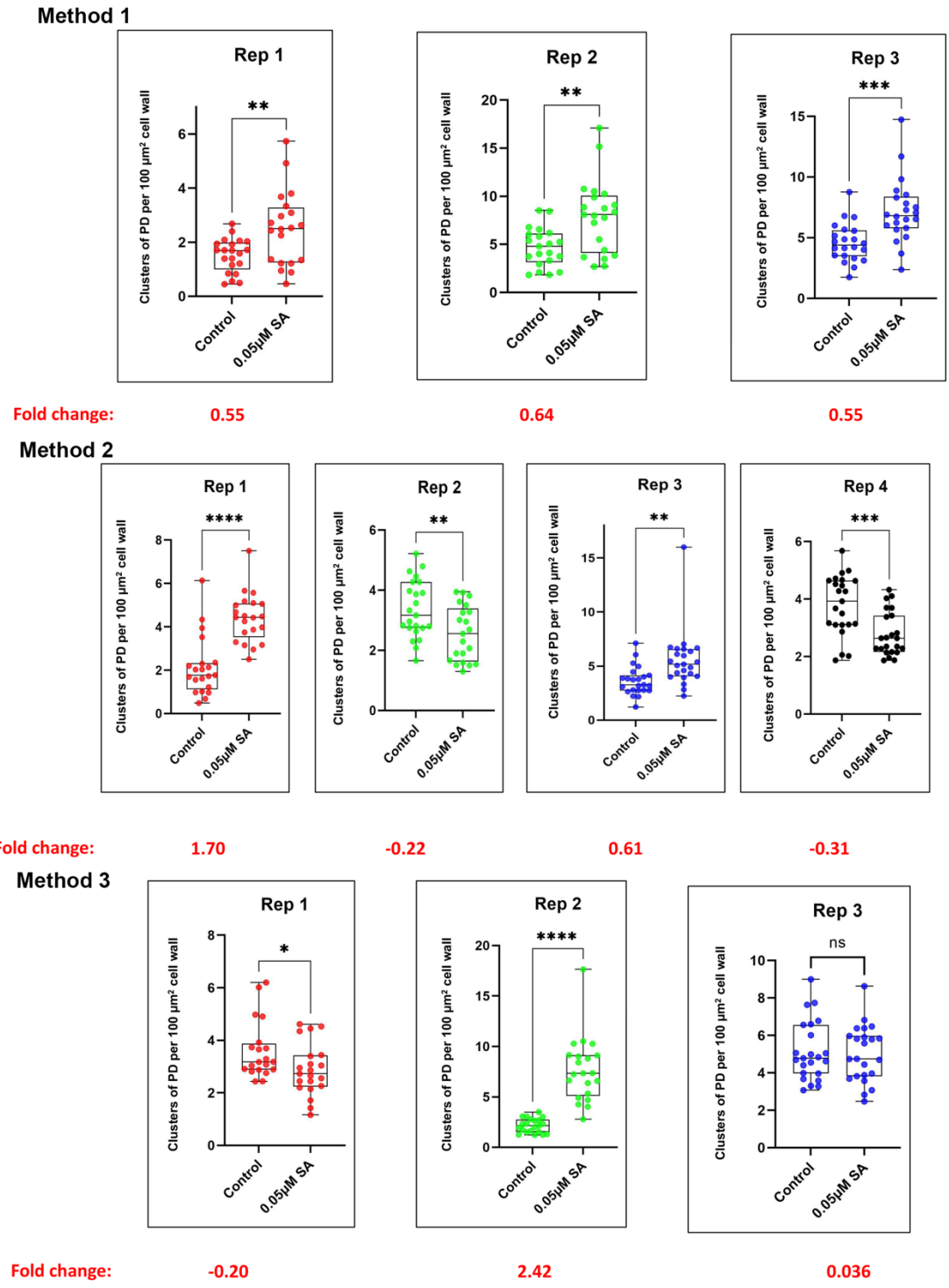

Fig. S3. Individual replicates for samples with or without treatment with SA. The fold change in the density of clusters of PD for each replicate is indicated before each graph. The data are the disaggregated data presented in Fig. 3 in the main text. Statistical analysis, Welch's t-test, was performed as described in the caption of Fig. 3.

Materials and Methods

Plant material and callose induction

The LAB strain of *Nicotiana benthamiana* was used in this study. Seedlings were germinated on soil for 7-10 days before transplanting to individual pots. *N. benthamiana* plants were grow on light carts under long day condition with 16 hours light (120 µmol m^{-2} s^{-1}) and 8 hours dark at 25 °C. Miracle Gro All-purpose Plant Food fertilizer was applied after 10-13 days post germination (3 days after transplanting). The leaves of 4-5 weeks old plants were used for callose quantification and salicylic acid treatment experiments.

Plasmodesmata callose staining and quantification.

Three methods were evaluated for identifying callose structures. All methods used 1% aniline blue (Ward's Science plus, Rochester NY LOT AD-22103) in 0.01 M K_3PO_4, pH 12 buffer. Method 1 was adapted from (Zavaliev and Epel, year) to image callose utilizing aniline blue on fixed tissues. Method 2 was adapted from John Innes Center (Aniline blue staining of quantification of plasmodesmal callose (jic.ac.uk)), and Method 3 was adapted from the Lee Lab University of Delaware[12]. For all three methods the 4th and 5th leaves of *N. benthamiana* were directly infiltrated with a 1mL syringe containing 1% aniline blue.

Method 1: Staining and sample preparation.

An entire cut leaf was submerged in 95-96% ethanol in a 500-mL polypropylene jar to bleach the tissue. The petiole was held with forceps to avoid mechanical damage to the

leaf. The jar was sealed, and samples were incubated at room temperature on a shaker at 30-40 rpm for at least 5 hours. The ethanol solution was changed to speed up the bleaching after 2 hours incubation. Incubation was continued until the leaves were completely or nearly completely bleached, but less than 6 hours, since plasmolysis occurs at this point, and the resulting separation of the plasma membrane and cell wall make it difficult to identify of clusters of PD. Bleached leaves were removed by gently holding by the petiole to avoid breaking the leaf and were placed in a petri dish and cut into 5 mm wide strips with a razor blade. The cut strips were rehydrated in double distilled water (DDW) with 0.01% Tween-20 and incubated at room temperature for 1 hour on a shaker at 30-40 rpm. Tissues were then transferred to a small petri dish (35mm in diameter and 10 mm heights) and submerged in aniline blue solution. The unlidded petri dish was placed in a house vacuum desiccator and vacuumed for approximately 10 minutes followed by slow release of pressure. The petri dish was covered and sealed with foil before shaking at room temperature for 2 hours at 30-40 rpm. No de-staining was necessary. The samples were then imaged with confocal microscopy.

Method 2: callose staining in unfixed tissue.

The 4^{th} and 5^{th} leaves of 4- to 5-weeks-old *N. benthamiana* plants were infiltrated with 1% aniline blue using a 1-mL needleless syringe. Leaves were then cut into 3-5mm strips and placed on a microscope slide for confocal microscopy.

Method 3: 1 hour aniline blue staining on unfixed tissue

The leaves of 4-5 weeks old *N. benthamiana* plants were cut into 5mm strips and incubated in 1% aniline blue in 0.01 M K_3PO_4, pH 12 buffer in the dark for 30-60 minutes. Aluminum foil was used to cover the petri dish containing the cut leaves and 1% aniline blue solution. After submerging leaf tissues in a staining solution, they were vacuumed gently for 10 minutes.

Confocal microscopy

A Leica SP8 laser scanning confocal scanning microscope (Leica, Whetzlar, Germany) was used to imaged callose deposits from the abaxial side of the leave tissues using a 40x/1.10 water immersion objective (HC PL APO CS2 40x/1.10 WATER). The excitation for aniline blue was with a 405-nm laser, UV (0.5-1%) and emission was captured from 415 nm-525 nm. Z-stacks were collected from multiple regions of interest (ROI) (approximately 23-25 ROIs per leaf) were collected. Z stacks were collected using the system optimized step size (<1 µm). All three methods were analyzed using ImageJ to quantify aniline blue-stained callose at plasmodesmata.

Scanning parameters and Acquisition settings

Frame scanning mode: XYZ

Frame size: 1024 x 1024

Zoom factor: 5

Line average: 1

Pixel depth: 8 bit

Scan speed: 400 Hz

To observe as many PD as possible, the pinhole aperture was initially set to open. Laser intensity and gain were adjusted to optimize the PD fluorescence against the background signal, while being careful to avoid oversaturation of callose sites. Saturation of the stomata was permitted. Twenty three to twenty five Z-stacks were imaged using the same settings of image acquisition in the independent experiments.

ImageJ analyses

For image analysis, the raw files were converted into max intensity Z-projections in ImageJ [13,14]. Images were converted into 8-bit grayscale, inverted, and threshold adjusted to identify pixels of clusters of PD and to reduce background noise for better analysis. Connected components in a binary image were separated by watershed separation. An automatic particle analysis was performed to obtain information on PD-associated callose particles. Clusters of PD per 100 μm^2 cell wall were calculated using Microsoft Excel.

Statistical analyses

Interquartile analysis was done in Excel by using the interquartile range method to remove outliers. Data were analyzed using GraphPad Prism 9 (version 9.5.0) and presented as Box & Whiskers plots with all values for clusters of PD. Plots display the middle line representing the median, 1-4 quartiles with the minimum and maximum values within the interquartile range. Clusters of PD per 100 μm^2 cell wall were

normalized to untreated control. An unequal variances Welch's t-test was conducted for each plot.

CalloseQuant and quantification

Semi-automated quantification of clusters of PD was performed using the CalloseQuant plugin developed by *C. Huang et al.* 2022. Images captured using confocal microscopy were first auto-scaled and converted into .tiff format using FIJI ImageJ[15]. Depending on the nature of the confocal micrograph, the peak prominence values range were between 25-45μm, and the measurement radius was maintained at 5.5 for Method A. For method B, the rolling ball radius range was used with 6-8 pixels, and the mean filter radius was kept at 2 pixels. The images were thresholded using Bremsen's technique at a radius of 50. Due to programming errors in Method B, the thresholded particles were manually analyzed at a micron size of 0.02-infinity with a circularity range of 0.00-1.00. All the data collected were manually checked for the elimination of signals and data points outside of the region of interest (ROI).

Salicylic acid treatment

N. benthamiana leaves were infiltrated with 0.05 mM salicylic acid (Sigma-Aldrich) prepared from a 100 mM stock solution in DMSO and diluted with distilled water.